ELSEVIER

Journal of Molecular Catalysis A: Chemical 192 (2003) 63–72

JOURNAL OF MOLECULAR CATALYSIS A: CHEMICAL

www.elsevier.com/locate/molcata

The interaction of *cis*-2-butene over a 10-ring Brönsted acid site of zeolite: a theoretical study

Humberto Soscun [a,*], Javier Hernández [a], Olga Castellano [a], Federico Arrieta [a], Fernando Ruette [b], Aníbal Sierralta [b], Francisco Machado [c], Marcos Rosa-Brusin [c]

[a] *Laboratorio de Química Inorgánica Teórica, Fac. Exp. de Ciencias, Departamento de Química, Ap. 526, Grano de Oro, Módulo No. 2, Maracaibo, Venezuela*

[b] *Centro de Química, IVIC, Ap. 21827, Caracas, Venezuela*

[c] *Escuela de Química, Universidad Central de Venezuela, Apartado 47102, Caracas 1020-A, Venezuela*

Accepted 6 March 2002

Abstract

We have investigated theoretically the interaction of *cis*-2-butene with a Brönsted acid site (BAS) embedded within a ring of 10 tetrahedral zeolite cluster (T10-OH). Calculations were performed at ab Initio SCF-MO level with the STO-3G basis set. Cs symmetry restriction was imposed for the optimization geometry of the T10-OH cluster, and no symmetry restriction was assumed for the *cis*-2-butene–HO-T10 interaction. This interaction first leads to the formation of a molecular complex, where the C=C is weakly coordinated to the proton of the BAS. Then, a hexa-cyclic transition state involving the coordination of one C atom of the C=C to one oxygen atom next neighbor of the OH group and the other C atom to the acid proton. Finally, an intermediate secondary alkoxy complex is formed. The alkoxide structure is a very stable complex, dominated by a covalent C–O bonding between the C atom and zeolite oxygen atoms.

Keywords: *cis*-2-Butene; Brönsted acid site; T10-OH cluster

1. Introduction

The reaction of isomerization of *n*-butene to produce isobutene proceeds with high selectivity and yield over a variety of medium pore zeolites. Ferrierite zeolite possessing a 10-ring and 8-ring pore system has been the subject of a great deal of work [1]. Both the strength and density of the Brönsted acid sites and the spaciousness of the channel system of this kind of zeolites, have been invoked as the reason for the high selectivity towards the isobutene formation. Two main mechanisms for this reaction have been proposed: (i) monomolecular and (ii) bimolecular. In the monomolecular mechanism, the direct isomerization of *n*-butene goes through the formation of a primary carbenium ion intermediate [2]. In the bimolecular one, the reaction begins with an oligomerization of *n*-butene to octene followed by cracking of the octene to isobutene [3]. In the latter case more cracking products, such as propene, pentene and hexenes, are expected [4]. By contrast the monomolecular mechanism should lead to a higher selectivity to isobutene as has

* Corresponding author. Tel.: +58-261-7598125; fax: +58-261-7317902.
E-mail address: hsoscun@sinamaica.ciens.luz.ve (H. Soscun).

1381-1169/02/$ – see front matter © 2002 Elsevier Science B.V. All rights reserved.
PII: S1381-1169(02)00118-8

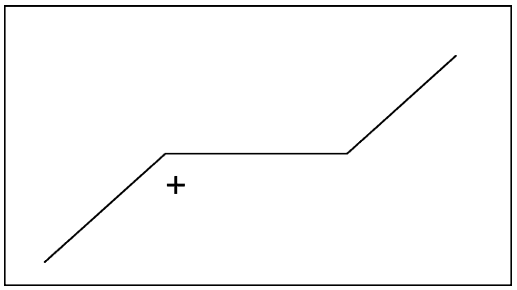

Fig. 1. Secondary C_4 carbenium ion.

been, in fact, observed. In addition to these statements, a pseudo-monomolecular mechanism has been also advanced in order to explain the coke participation in the selective skeletal isomerization of *n*-butene [1g].

Recently, a very interesting work, aimed to identify the precursor species of the butene–isobutene conversion over H-ferrierite, was carried out using IR and UV–Vis spectroscopies [5a]. This study showed that the isomerization of 1-butene to 2-*cis*, and 2-*trans*-butene occurs through a bimolecular route in the temperature range from 300 to 673 K. A relevant feature from this study is the proposal of a secondary carbenium ion C_4 (Fig. 1) charged species [5b], obtained by butene protonation, followed by the formation of an alkoxide-like saturated-chain intermediate bonded to the zeolite framework by a bond having a prevalently covalent character [5]. All seems to point out towards the fact that the molecular route to isobutene depends mainly upon the temperature and the acid sites concentration. Thus, high temperatures (ca. 773 K) and high Si/Al ratios favors the monomolecular mechanism, whereas the bimolecular one is facilitated at the opposite conditions (low Si/Al ratios and low temperatures) [1]. However, it is important to note that the experimental conditions of the reaction (reaction temperature, *n*-butene partial pressures, etc.) also influence the activity and selectivity of the particular H-ferrierite employed for the isomerization of butenes [1g]. For example, high selectivity to isobutene formation has been found over H-ferrierite with low Si/Al ratio at high temperatures (ca. 623 K) [1g] without the expectation of an explicit monomolecular mechanism. In this sense, a great deal of experimental work has been reported in order to gain insight into the details of the proposed isomerization mechanisms [1].

At theoretical level, the mechanism of the isomerization reaction of *n*-butene in zeolites has been studied by Boronat et al. [6]. These authors have used the density functional theory [7] to carried out their calculations, where for the zeolite model was used the $H_3Si(O)AlH_2(OH)SiH_3$ cluster (T3) (Fig. 2), which consists of two Si and one Al tetrahedral [6]. It was found that the double bond isomerization goes to a concerted mechanism, where the OH hydroxyl group of the zeolite protonates the double bond of 1-butene and the neighboring O atom abstracts a hydrogen from the olefin, restoring the zeolite active site and giving the adsorbed 2-butene. Additionally, for the skeletal isomerization of 1-butene a three steps mechanism was proposed. The first one involves the protonation of the adsorbed 1-butene to give a secondary alkoxy intermediate. Then, this alkoxy is converted to a branched primary alkoxide through a cyclic transition state, and finally desorption of the primary alkoxide occurs to give isobutene. These alkoxide intermediates consist of C_4 charged species bonded to the O atom neighboring to the BAS.

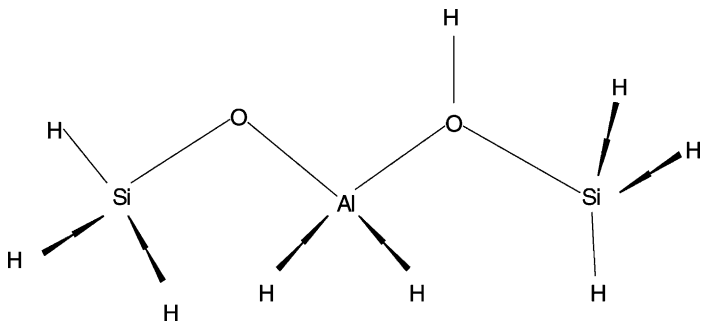

Fig. 2. T3 zeolite cluster.

These results obtained with small zeolite clusters are good starting point for understand at electronic level the main interactions that dominate the reaction mechanisms in zeolites. However, for a complete description of the overall interactions between the interacting molecule and a zeolite system, the real zeolite structure need to be approached by an accurate representation of the zeolite model. This aspect has to be very well addressed because that besides to the absorption process, additional interactions between the sorbate and different zeolite atomic sites from the zeolite environment are also able to occur.

In the present work, we report a theoretical investigation about the chemical interaction of *cis*-2-butene molecule with a model of 10-member-ring zeolite cluster, consisting of nine silicon atoms, one aluminum tetrahedral (Si/Al = 9) and one BAS, designated as T10-OH (10 M-R) as shown in Fig. 3. This cluster was theoretically constructed with the aim of representing the Brönsted acid activity of the OH group in ferrierites and similar 10 M-R. Furthermore, this T10 cluster is able to give different interactions with the *cis*-2-butene molecule in order to gain insight in the mechanism of skeletal isomerization of butenes in 10 M-R zeolites. This study includes full geometry optimization of the T10-OH cluster, the *cis*-2-butene molecule, and the complete T10-OH–*cis*-2-butene interaction. This interaction leads to the formation of an stable secondary C_4 alkoxide through an adsorbed *cis*-butene–zeolite complex. Further calculations are to be done to consider an ulterior stage involving methyl jump and proton transfer from the alkoxide intermediate to the zeolite cluster to form isobutene and to restore the BAS.

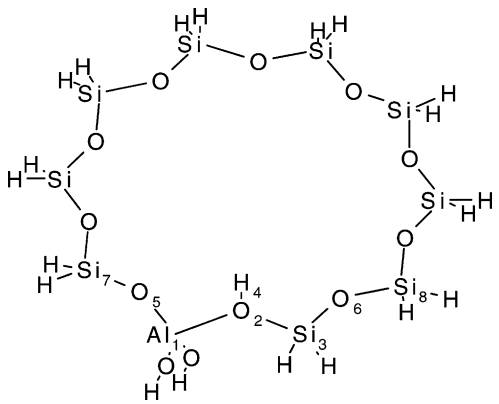

Fig. 3. Structure of T10-OH zeolite cluster.

2. Calculation details

In this work, we have constructed a T10-OH ring for modeling the active site of the ferrierite and 10 M-R zeolite structures. This 10-ring is formed by one Brönsted acid site hydroxyl group and nine silicon atoms linked with O atoms and saturated with H atoms, where the structural formula of this cluster is $(SiH_2)_9(O)_9Al(OH)$ with Cs symmetry. The calculations for the T10-OH–*cis*-2-butene interaction started by approaching the *cis*-2-butene molecule to the BAS region of the zeolite cluster without imposing symmetry restriction. This condition was followed in order to allow freedom to the *cis*-2-butene molecule into the T10-ring, because it has been shown from adsorption studies and Monte-Carlo simulations that the reaction between a sorbate molecule and the zeolite structure is not restricted to only one ring [8]. The full geometry optimization of the complex interaction were performed at Hartree–Fock level and the STO-3G basis set [9]. It is important to note that STO-3G is a minimum basis set, and is not accurate enough for energetic calculations, however, according to the size of the system is a good starting point for the structural studies of the zeolitic system we are dealing with.

In the optimization geometry process, the initial stage or intermediary of the interaction between T10-OH and the *cis*-2-butene is a molecular adsorption complex between the T10-OH cluster and the double bond –C=C– of the *cis*-2-butene, where this double bond interacts directly with the H atom of the BAS oz zeolite; and the following step leads to the formation of a cyclic 6-member transition state structure. The final product is the carbenium ion C_4 secondary alkoxide, referred as T10-O-*sec*-butyl compound. This final complex was further optimized with the 3-21G* basis set [10] at Hartree–Fock level and then was optimized by using density functional theory DFT [7] with the B3LYP [11] hybrid approach and the 3-21G* basis set. This DFT methodology account for the exchange and correlation electronic effects, that are significant for the interaction were bonds are broken and new ones are formed. These calculations were performed for estimating more accurately

the energies and the structures of the stable final species.

All calculations were carried out with the Gaussian 98 [12] suite of program on Silicon Graphics Origine 2000 workstations.

3. Results and discussions

3.1. Geometric structures, energetic and charge distribution

For the present work, we have fully optimized a Cs structure of 10 tetrahedral zeolite ring with only one Brönsted acid site that is designated as T10-OH cluster. The optimization of this ring has been performed at the HF/STO-3G level of theory, and the relevant geometric parameters are shown in Fig. 5. The main features of this structure, the O–H, Si–O and Al–O length bonds and the H–Si–O, O–Si–O, Al–O–Si and Si–O–Si bond angles, are reported in Table 1. Because of ferrierite is an excellent catalyst for the isomerization of *n*-butene to isobutene, we compare the structural features of the optimized T10-OH cluster with those of ferrierite experimental structure. The ferrierite is a zeolite that can be found in natural form and can be also synthesized. The structure of a natural ferrierite Mg-rich material was determined by X-ray data by Vaughan [13a] and later the structure of the siliceous ferrierite was reported by Weigel et al. [13b]. The network of this zeolite is based on 5-ring building units, forming 10-ring channels with diameters of $5.4 \times 4.2\ \text{Å}^2$, that are interconnected by cages with 8-ring channels, which pore diameters are of

Table 1
Relevant optimized geometric parameters of *cis*-2-butene, T10-OH, *cis*-2-butene–HO-T10 and *sec*-2-butyl–O-T10 complexes

	cis-2-Butene	T10-OH	*cis*-2-Butene–HO-T10	TS	*sec*-Butene–O-T10
Bond distances (Å)					
C_1–C_2	1.524		1.521, 1.496[a]	1.557	1.549, 1.514[b]
C_2–C_3	1.312		1.522, 1.497[a]	1.542	1.556, 1.519[b]
C_3–C_4			1.314, 1.343[a]	1.541	1.549, 1.524[b]
Al_1–O_2		1.931, 1.626[c]	1.766, 1.970[a]	1.786	1.720, 1.741[b]
O_2–Si_3		1.697, 1.469–1.731[d]	1.741, 1.701[a]	1.617	1.653, 1.630[b]
O_2–H_4		0.950	0.970, 0.994[a]	1.266, 1.219[e]	
Al_1–O_5		1.718, 1.626[c]	1.645, 1.745[a]	1.625	1.661, 1.991[b]
Si_3–O_6		1.621, 1.613[c], 1.469–1.731[d]	1.676	1.746	1.966
O_5–Si_7		1.603	1.619, 1.637[a]	1.577	1.612, 1.707[b]
O_6–Si_8		1.638	1.627	1.720	1.705
H_4–C_2			2.572, 2.162[a]		
H_4–C_3			2.636, 2.097[a]	1.274	
C_2–O_6				1.464	1.446, 1.477[b]
Bond angles (°)					
C_3–C_2–C_1	124.7		128.0	128.7	113.8
Al_1–O_2–Si_3		127.4	107.6, 127.3[a]	122.8	100.7, 149.8[b]
O_2–Si_3–O_6		105.0, 109.5[c], 97.7–120.9[d]	88.4	99.1	89.8
O_5–Al_1–O_2		97.2, 109.5[c]	113.1, 96.3[a]	100.8	118.7, 102.5[b]
Si_3–O_2–H_4		119.2	118.6, 118.1[a]	129.3	
Si_3–O_6–Si_8		146.4, 148.2–157.9[c], 148.2–168.6[d]	129.3	122.7	122.7
Al_1–O_5–Si_7		148.6, 153.6[c]	134.1, 146.4[a]	173.2	133.5, 115.6[b]
O_6–C_2–C_3				108.7	136.1
H_4–C_3–C_2				109.3	
Si_3–O_6–C_2					116.3, 117.4[b]

[a] Calculated structure for 2-butene and T3 zeolite cluster, Ref. [5].
[b] Calculated structure for the secondary alkoxy intermediate between 2-butene and T3, Ref. [5].
[c] Relevant geometric parameters on the zeolite ferrierite [13a].
[d] Relevant geometric parameters on the siliceous ferrierite [13b].
[e] Calculated distance in transition state from olefin chemisorption [17].

4.8 × 3.5 Å^2. The diameter of the cages is about 7 Å. The relevant experimental geometric parameters for the ferrierite structure and the siliceous one are reported also in Table 1. These values show that the theoretical Si–O, Al–O, Si–O–Si and Al–O–Si bond features of the T10-OH cluster are within the range of the experimental determined parameters in the real zeolite, with the exception of the Al–O bond distance, which value in T10-OH is 1.931 Å, and in the ferrierite is about 1.626 Å. This difference in about 0.30 Å can be explained in terms that the strength of the Al–O bond in real zeolites are increased by the effects of the crystal electrostatic interactions. These interactions produce a shortening of the corresponding bonds. With respect to the size of the T10-OH ring, was found that their dimensions are 8.05 × 7.65 Å^2, and considering the value of 1.4 Å as the van der Waals radius of oxygen, the diameter of this pore is 5.25 × 4.85 Å^2. These results show that the optimized T10-OH ring is slightly bigger in about 2.80 Å^2 than the corresponding to a 10 M-R ferrierite. In general, the structural pattern between the T10-OH cluster and ferrierite, and similar 10-membered zeolite rings is good enough for the calculations presented here.

For consistency reasons, we have also optimized the geometry of *cis*-2-butene, which HF/STO-3G relevant parameters are depicted in Fig. 4. The interaction of *cis*-2-butene with the T10-OH zeolite cluster is dominated by a bonding between the C=C of *cis*-2-butene and the proton of the OH hydroxyl group of the zeolite, giving the π-adsorption complex (*cis*-2-butene–HO-T10) that is shown in Fig. 6. Fig. 6a shows the details of optimized structural parameters in the region of the interaction and Fig. 6b shows a full view of the absorption structure of the *cis*-2-butene molecule into the 10 M-R zeolite model. In addition, the relevant optimized geometric parameters of *cis*-2-butene–HO-T10 complex structures are also displayed in Table 1. The details of the local structure of this complex are in agreement with

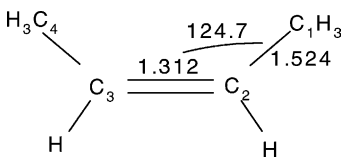

Fig. 4. *cis*-2-Butene structure.

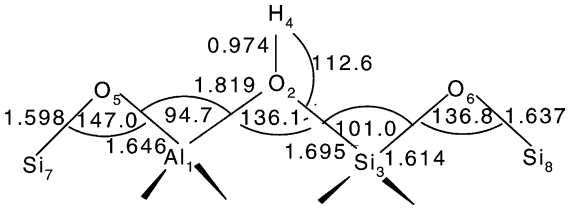

Fig. 5. HF/STO-3G optimized geometric parameters of the BAS of T10-OH zeolite cluster.

previous theoretical results [6,14,15]. How there was not symmetry restriction for the complex optimization, was found that the adsorption of the c*is*-2-butene molecule produces a significant distortion in the T10 ring, forcing the Si(OH)Al moiety to move the OH hydroxyl group out of the plane of the T10 zeolite, and the organic frame is out of the ring plane as well. A cause of this interaction, the zeolite structure is hardly perturbed during the formation of the *cis*-2-butene–HO-T10 complex, particularly the bonds close to the BAS. Comparing the geometric parameters depicted in Fig. 5 (Table 1) with the corresponding ones in Fig. 6 (Table 1), significant geometric variations resulting from the perturbation of the *cis*-2-butene molecule can be observed. In particular, it is important to note the shortening of the Al_1–O_2, Al_1–O_5, and the increasing of the C_2–C_3, O_2–Si_3, O_2–H_4, Si_3–O_6 and O_5–Si_7 bonds. The OH acid bond length varies from 0.950 to 0.970 Å. Additionally, important perturbations occurs with the bond angles around the acid site, such as the Al_1–O_2–Si_3, which value from the isolated cluster switching from 136.1° to 107.6° in the complex. The latter value is very close to the optimum T–O–T bond angle of 109.5° expected for the tetrahedral angles between hybrid sp^3 orbitals. It means that the zeolite cluster acquires stability by interacting with *cis*-2-butene to form the complex shown in Fig. 6. The O_5–Al_1–O_2 also approaches to the optimum tetrahedral angles by passing from 94.7° to 113.1°. As a result of the previous angles modifications, a smaller change in the Si_3–O_2–H_4 angle from 112.6° to 118.6° also occurs. Similar variations in the zeolite structure have been reported for the theoretical calculation of the interaction of 2-butene with a T3 zeolite cluster [6]. The relevant geometric parameters of these calculations are also reported in Table 1 for comparison.

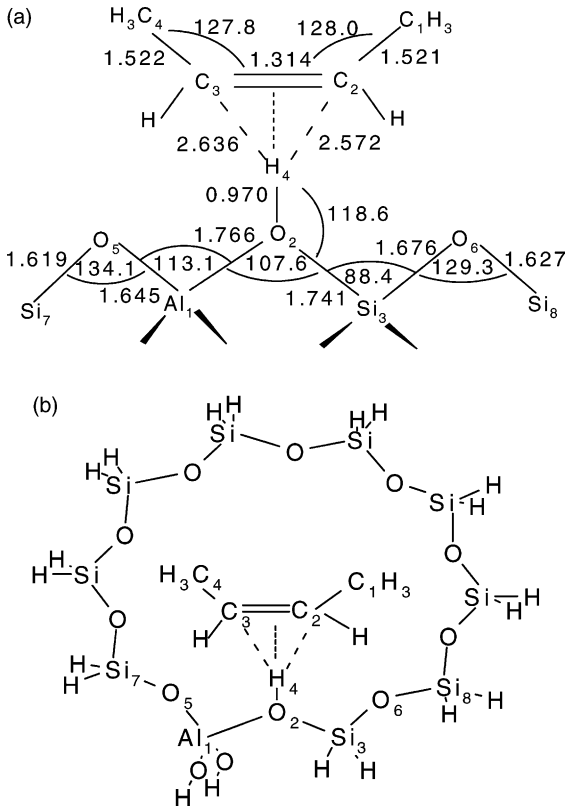

Fig. 6. (a) Local details of the adsorption π-complex structure (*cis*-2-butene–HO-T10) of the interaction of *cis*-2-butene and T10-OH zeolite cluster; (b) full view of the adsorption π-complex structure (*cis*-2-butene–HO-T10).

How was mentioned, because of the *cis*-2-butene adsorption, and by steric repulsion of this molecule with the rest of the ring, the BAS is moved to lies out of the ring plane and in consequence no important interactions between the sorbate and the adjacent oxygen atoms to the BAS of the T10 M-R are present. These results suggest that the formation of the π-complex in the real zeolite must be located in the zeolite cages where more space it is available, and not restricted to a particular window channel. At this point it is important to analyze the adsorption and diffusion of hydrocarbon in zeolites. In this context, Jousse et al. [16] have been reported significant studies about molecular dynamic simulation of the interaction of butene isomers in different zeolite structures. These authors have shown that the interactions between butenes and zeolites can be explained in terms of confinement effects and the shape complementarity between them. In particular, it was found that the minimum energy for the butenes adsorption in ferrierite is reached when these molecules are located at the intersection of the zeolite channels, with distortion of the BAS network [16]. Our results are in agreement with these studies about the tendency of the *cis*-butene molecule to goes out of the ring zeolite plane.

Table 2 report the values of the total energies E_T of the involved species at the HF level. With this level of theory, the calculated binding energy (E_b) for the *cis*-2-butene–HO-T10 complex is about −54.7 kcal/mol. In spite of the fact that the absolute value of this calculation is far from reality, the negative value the binding energy indicates that the interaction of *cis*-2-butene with the zeolite cluster is of adsorptive character as has been found for theoretical studies of ethane [14,15], 2-butene [6] and molecular dynamic calculations, which interaction energy is −11.07 kcal/mol [16].

Further interaction of 2-*cis*-butene with the zeolite cluster leads to the formation of the transition state (TS) shown in Fig. 7. The part (a) of this figure shows a local view of the TS structure and details of the relevant optimized geometric parameters, whereas Fig. 7b shows a general picture of the location of the TS into the T10 M-R zeolite. Relevant optimized geometric parameters of this TS calculation are also quoted in Table 1. The structure of this transition state shown in Fig. 7 consists of a 6-member cycle in which the atoms O_2–H_4–C_3–C_2–O_6–Si_3 are the vertices of the hexagon. The nature of transition states related to processes of hydrocarbon conversion, including the adsorption of olefins, have been studied by Rigby et al. [17] by using quantum mechanic methods. These authors have found that these TS involve five or six ring structures formed between the O–Al–O atoms of the zeolite clusters and two or three C or H atoms of the organic compound. These findings have been verified by Boronat et al. [6] and more recently by Senger et al. [15]. In our model, we have found similar TS structure, but the six ring structure is formed between the O–Si–O atoms and the two C atoms of the hydrocarbon. Structurally, these TS are similar in nature. For instance, the calculated distance between the O atom of the zeolite moiety and the transferring H, O_2–H_4, is 1.266 Å (see Fig. 7a), whereas it is 1.219 Å for the corresponding to the

Table 2
Total energies E_T (Hartree), binding energy E_b (kcal/mol), activation energy E_a (kcal/mol), energy for the process of formation of the alkoxide complex E_f, and relevant atomic charges (Q/e) of *cis*-2-butene, T10-OH, *cis*-2-butene–HO-T10 and *sec*-2-butyl–O-T10 complexes

	cis-2-Butene	T10-OH	*cis*-2-Butene–HO-T10	TS	*sec*-Butene–O-T10
E_T	−154.241981, −155.242057[a], −156.368447[b]	−3708.481528, −3735.117329[a], −3745.244791[b]	−3862.8106723	−3862.693877	3862.831929, −3890.431438[a], −3901.700161[b]
E_b			−54.7		
E_a				18.6	
E_f					−68.3, −23.7[c], −45.2[a], −54.5[b]
Q/e					
C_1	−0.187		−0.189	−0.220	−0.205, −0.194[d], −0.655[e], −0.570[f]
C_2	−0.060		−0.077	+0.093	+0.086, +0.083[d], +0.052[e], 0.025[f]
C_3	−0.060		−0.081	−0.187	−0.123, −0.101[d], −0.504[e], −0.368[f]
C_4	−0.187		−0.207	−0.191	−0.179, −0.180[d], −0.605[e], −0.568[f]
Al_1		+1.190	+1.235	+1.185	+1.163, +1.182[e]
O_2		−0.508	−0.539	−0.600	−0.670, −0.797[e]
Si_3		+1.067	+1.107	+1.017	+1.015, +1.284[e]
H_4		+0.255	+0.248	+0.212	
O_5		−0.727	−0.701		
O_6		−0.652	−0.684	−0.473	−0.448, −0.812[e], −0.551[f]
Si_7		+1.035			
Si_8		+1.063		+1.119	+1.050, +1.050[e]

[a] HF/3-21G* (this work).
[b] B3LYP/3-21G* (this work).
[c] DFT value for the formation of 2-butyl in a T3 zeolite cluster, Ref. [6].
[d] HF/STO-3G values of the *sec*-butenol molecule.
[e] HF/3-21G* atomic charge values with HF/3-21G* optimized geometry.
[f] HF/2-21G* atomic charge values of the *sec*-butenol with HF/3-21G* optimized geometry.

olefin chemisorption with the formation of a O–Al–O TS ring [17].

In the formation of the TS of Fig. 7, the energetic exigencies are lowered because of one oxygen atom adjacent to the hydroxyl group has the possibility of interacting with one C atom of the C=C of *cis*-2-butene. In fact, Table 2 contains the total energy value for this TS, that using as references the energy of the cluster and the isolated *cis*-2-butene, the corresponding activation energy (E_a) is about 18.6 kcal/mol. This value is in concordance with theoretical values of different TS from the interaction between butenes and zeolite clusters [6], and it is also consistent with the range of activation energy values of reaction mechanisms for hydrocarbon conversion in zeolites [17].

The following and last step that we have considered in the present work is the formation of the saturated-chain alkoxide intermediate shown in Fig. 8, by breaking the H_4–O_2 bond and consolidating the C_2–O_6 bond. This kind of intermediate was also invoked by Pazé et al. [5] to explain the formation of saturated hydrocarbon during the transformation of 1-butene. Fig. 8a shows the details of the alkoxide and zeolite structure, and Fig. 8b shows a full vision of the alkoxide species linked to the 10 M-R zeolite. Relevant geometric parameters are inserted in Fig. 8 and quoted in Table 1. These results are similar to other theoretical ethene–zeolite calculations. In particular, the interaction of linear butanes [6] and ethylene [14,15] with T3 cluster lead to the formation of intermediate alkoxides with similar structures, where the complex is dominated by the formation of a C–O bond. In the present work, we have calculated the length of the C–O bond as to be 1.446 Å. The corresponding reported lengths for ethyl-zeolite [15] is 1.469 Å and for the 2-butyl-zeolite [6] is 1.477 Å, that are in good agreement with our results. Table 1 also shows the relevant geometric parameters obtained for the secondary alkoxy intermediate in Ref. [6]. Despite of the differences in the level of calculations performed in Ref. [6]

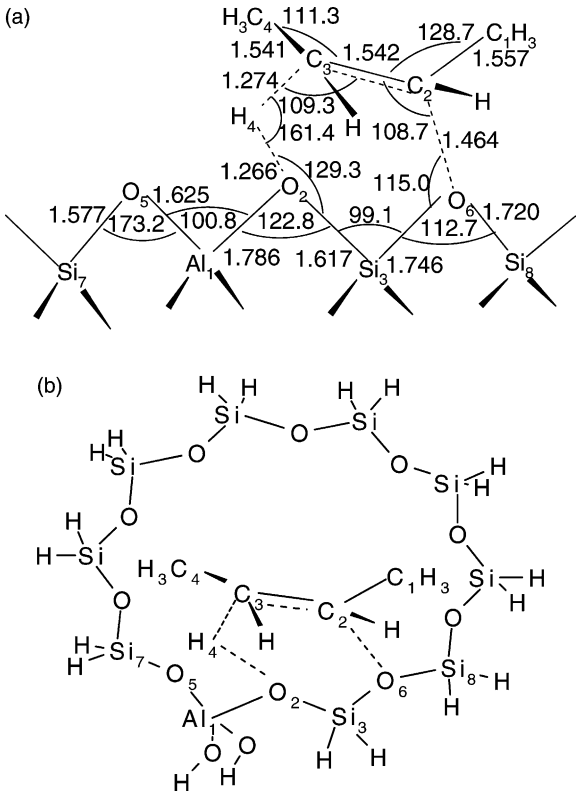

Fig. 7. (a) Transition state of the conversion of *cis*-2-butene to the *sec*-2-butyl over the T10-OH zeolite cluster (6-membered ring TS); (b) full view of the 6-membered ring transition state of the conversion of *cis*-2-butene to the *sec*-2-butyl over the T10-OH zeolite cluster.

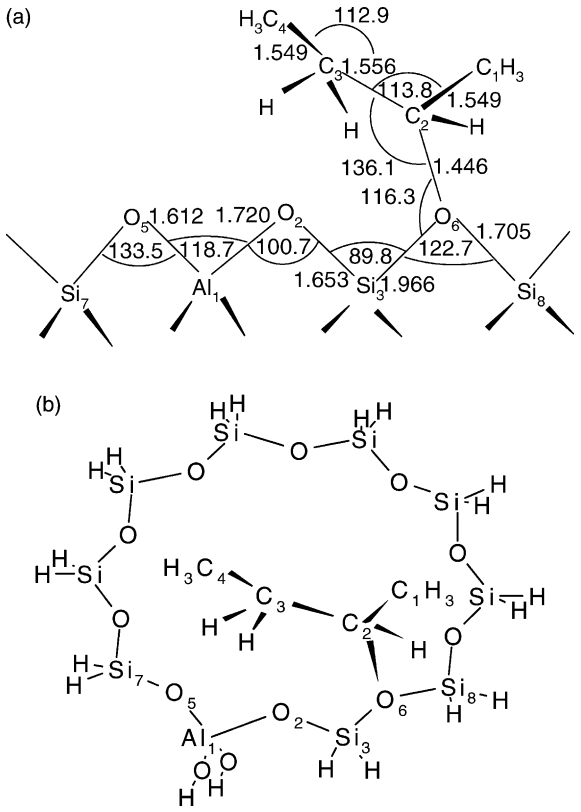

Fig. 8. (a) Structure of the T10-OH–*sec*-2-butyl complex (intermediate alkoxide); (b) full view of the structure of the T10-OH–*sec*-2-butyl complex (intermediate alkoxide).

(ab Initio and DFT calculations with an extended basis set), the agreement with our results is remarkable.

The total energy for the alkoxy complex structure it is also depicted in Table 1, and the formation energy (E_f) of the *sec*-butene–O-T10 alkoxy complex, calculated taking as reference the isolated T10-OH cluster and the *cis*-2-butene species, has a value of −68.3 kcal/mol as compared with −23.7 kcal/mol obtained for the case of the 2-butyl-T3 cluster [6]. The differences are due to deficiencies in the basis sets, the methods and the kind of zeolite cluster. Further optimization calculations at the HF/3-21G* and B3LTP/3-21G* levels were performed for the involved species in the formation of the *sec*-butene–O-T10 alkoxy complex, which values of total energies are also reported in Table 1. These energies give for the process of alkoxide formation the values of −45.2 and −54.5 kcal/mol, respectively.

3.2. Atomic charges

The atomic charges from the Mulliken analysis of the species involved in the interaction *cis*-2-butene–T10-OH are shown in Table 2. These figures can only be used as a reasonable reference because they change with the method employed and the basis sets, and cannot be experimentally verified for molecules, but can be evaluated experimentally from X-ray determinations in crystal structures [18]. However, in the present work Mulliken atomic charges are very useful for understanding at electronic level the changes occurring in both the zeolite cluster and the *cis*-2-butene molecule as a result of their mutual interaction leading

to the formation of the alkoxide intermediate. In the initial adsorption process for the formation of the *cis*-2-butene–OH-T10 structure of Fig. 6, the atomic charges on the C atoms of the *cis*-2-butene adsorbed on the zeolite atoms, resemble those of the isolated olefin and the isolated zeolite. No significant variations in these charges were observed. However, the formation of the transition sate of Fig. 7, important changes were observed in the atomic charges of C_2 and in the O_6 atoms. C_2 is the carbon atom changing from sp^2 to sp^3 hybridization and its electron charge is being partially transferred to atom C_3, i.e., in turn, receiving the acidic proton from the zeolite. In this case, the positive charge is concentrated on the C_2 atom of the organic fragment, how has been verified by van Santeen and coworkers [17]. Additionally, O_6 becomes less negative as a result of the formation of the O_6–C_2 bond. Simultaneously, the atom O_2, as expected, increases its negative charge. For the rest of the atoms, only small variations are observed in the atomic charge distribution.

For the formation of the alkoxy complex the tendencies observed during the TS formation, previously described, are maintained. In Table 2, the values of the atomic charges at the HF/3-21G* level for this complex are also presented. The variations are evident between the HF/STO-3G and HF/3-21G* charges, but the tendencies in the charge transference remain the same. Similar pattern for these charges has been reported elsewhere [6]. Additionally, atomic charges of the *sec*-butenol molecule calculated using HF/STO-3G and HF/3-21G* are also given in Table 2 for comparison purposes. It seems to be clear the similarities between the *sec*-butenol molecule and the alkoxide complex. This charge distribution study also suggests that the nature of the alkoxide–zeolite bond is prevalently covalent, in agreement with previous findings [6,17].

4. Conclusions

The interaction between *cis*-2-butene with a zeolite 10-membered ring acid site, has been investigated by theoretical calculations performed at ab Initio SCF-MO level with the STO-3G basis set. A Brönsted site embedded within a 10-tetrahedral ring-cluster (T10-OH) was used as a the zeolite model. For the optimization geometry of the T10-OH cluster Cs symmetry restriction was imposed. For the *cis*-2-butene–HO-T10 interaction no symmetry restriction was assumed. It was first observed the formation of an adsorbed molecular complex where the C=C of the *cis*-2-butene is coordinated to the BAS trough a Π-like adduct. Then, further interaction leading to a secondary alkoxy complex occurred. This alkoxide species was formed through a cyclic 6-membered O–Si–O transition state TS. In this cycle the hydrogen atom, the oxygen of the OH group and the one adjacent to it, the framework Si atom between both oxygen atoms and the two C atoms of the C=C, conform the vertices of the resulting hexagon. Calculations have shown hat the alkoxy intermediate is a very stable complex dominated by a covalent C–O bonding. The study of the interaction energy, activation energy, the formation of the alkoxy complex, and the atomic charge distribution results are in agreement with previous theoretical calculations.

Acknowledgements

The authors thank to the CONICIT of Venezuela for financial support under the grants S1-95001617 and CONIPET No. 97003734.

References

[1] (a) H.H. Mooiweer, K.P. de Jong, B. Kraushaar-Czarnetski, W.H.J. Stork, B.C.H. Krutzen, Stud. Surf. Sci. Catal. 84 (1994) 2327–2334;
(b) K.P. de Jong, H.H. Mooiweer, J.G. Buglass, P.K. Maarsen, Stud. Surf. Sci. Catal. 111 (1997) 127–138;
(c) W.Q. Xu, Y.G. Yin, S.L. Suib, J.C. Edwards, C.L. O'Young, J. Phys. Chem. 99 (1995) 9443;
(d) J. Houzvicka, S. Hansildaar, V. Ponec, J. Catal. 167 (1997) 273–278;
(e) M. Guisnet, P. Andy, N.S. Gnep, E. Benazi, C. Travers, J. Catal. 158 (1996) 551–560;
(f) M.A. Asenzi, A. Martinez, Appl. Catal. A 183 (1999) 155–165;
(g) L. Domokos, L. Lefferts, K. Seshan, J.A. Lercher, J. Catal. 197 (2001) 68–80.
[2] C.L. O'Young, R.J. Pellet, D.G. Casey, J.R. Ugolini, R.A. Sawicky, J. Catal. 151 (1995) 467.
[3] M. Guisnet, P. Andy, N.S. Gnep, E. Benazzi, C. Travers, J. Catal. 158 (1996) 551.
[4] D. Rutenbeck, H. Papp, D. Freude, W. Schwieger, Appl. Catal A: 206 (2001) 57.
[5] (a) C. Pazé, B. Sazak, A. Zecchina, J. Dwyer, J. Phys. Chem. B 103 (1999) 9978;

(b) D.M. Brouwer, Chemistry and Chemical Engineering of Catalytic Processes, in: R. Prins, G.C.A. Schuit (Eds.), NATO ASI series, Series E, Appl. Sci. No. 39, Sithoff & Noordhoff, 1980, p. 137.
[6] M. Boronat, P. Viruela, A. Corma, J. Phys. Chem. A 102 (1998) 982.
[7] R.G. Parr, W. Yang, Density-functional Theory of Atoms and Molecules, Oxford University Press, Oxford, 1989.
[8] F. Eder, J.A. Lercher, Zeolites 18 (1997) 75;
W.J.M.J. van Well, X. Cottin, J.W. de Haan, B. Smit, G. Nivarthy, J.A. Lercher, J.H.C. van Hooff, R.A. van Santeen, J. Phys. Chem. B 102 (1998) 3945.
[9] W.J. Hehre, R.F. Stewart, J.A. Pople, J. Chem. Phys. 51 (1969) 2657.
[10] J.S. Binkley, J.A. Pople, W.J. Hehre, J. Am. Chem. Soc. 102 (1980) 939.
[11] A.D. Becke, J. Chem. Phys. 98 (1003) 5648;
C. Lee, W. Yang, R.G. Parr, Phys. Rev. B 37 (1988) 785.
[12] M.J. Frisch, G.W. Trucks, H.B. Schlegel, G.E. Scuseria, M.A. Robb, J.R. Cheeseman, V.G. Zakrzewski, J.A. Montgomery Jr., R.E. Stratmann, J.C. Burant, S. Dapprich, J.M. Millam, A.D. Daniels, K.N. Kudin, M.C. Strain, O. Farkas, J. Tomasi, V. Barone, M. Cossi, R. Cammi, B. Mennucci, C. Pomelli, C. Adamo, S. Clifford, J. Ochterski, G.A. Petersson, P.Y. Ayala, Q. Cui, K. Morokuma, D.K. Malick, A.D. Rabuck, K. Raghavachari, J.B. Foresman, J. Cioslowski, J.V. Ortiz, A.G. Baboul, B.B. Stefanov, G. Liu, A. Liashenko, P. Piskorz, I. Komaromi, R. Gomperts, R.L. Martin, D.J. Fox, T. Keith, M.A. Al-Laham, C.Y. Peng, A. Nanayakkara, C. Gonzalez, M. Challacombe, P.M.W. Gill, B. Johnson, W. Chen, M.W. Wong, J.L. Andres, C. Gonzalez, M. Head-Gordon, E.S. Replogle, J.A. Pople, Gaussian 98, Revision A.7, Gaussian, Inc., Pittsburgh, PA, 1998.
[13] (a) P.A. Vaughan, Acta Cryst. 21 (1966) 983;
(b) S.J. Weigel, J.-C. Gabriel, E. Gutierrez, A.B. Monge, N.J. Henson, L.M. Bull, A.K. Cheetham, J. Am. Chem. Soc. 118 (1996) 2427.
[14] Z. Guilling, L. Gang, D. Baiqing, J. Mol. Catal. A 147 (1999) 33.
[15] A. Senger, L. Radom, J. Am. Chem. Soc. 122 (2000) 2613.
[16] F. Jousse, L. Leherte, D.P. Vercauteren, J. Mol. Catal. A 119 (1997) 165.
[17] A.M. Rigby, G.J. Kramer, R.A. van Santeen, J. Catal. 170 (1997) 1.
[18] P.R. Mallinson, K. Wozniak, C.C. Wilson, K.L. MacCormack, D.S. Yufit, J. Am Chem. Soc. 121 (1999) 4640.